



Greenwich Academic Literature Archive (GALA)
– the University of Greenwich open access repository
<http://gala.gre.ac.uk>

Citation for published version:

Szilágyi, Petra Ágota, Weinrauch, Ingrid, Juan-Alcaniz, Jana, Serra-Crespo, Pablo, Grzech, Anna, Oh, Hyunchul, de Respinis, Moreno, Trzesniewski, Bartek Jacek, Kapteijn, Freek, van de Krol, Roel, Geerlings, Hans, Gascon, Jorge, Hirscher, Michael and Dam, Bernard (2014) Interplay of Linker Functionalization and Hydrogen Adsorption in the Metal–Organic Framework MIL-101. *Journal of Physical Chemistry C*, 118 (34). pp. 19572-19579. ISSN 1932-7447 (Print), 1932-7455 (Online) (doi:10.1021/jp5050628)

Publisher's version available at:

<http://dx.doi.org/10.1021/jp5050628>

Please note that where the full text version provided on GALA is not the final published version, the version made available will be the most up-to-date full-text (post-print) version as provided by the author(s). Where possible, or if citing, it is recommended that the publisher's (definitive) version be consulted to ensure any subsequent changes to the text are noted.

Citation for this version held on GALA:

Szilágyi, Petra Ágota, Weinrauch, Ingrid, Juan-Alcaniz, Jana, Serra-Crespo, Pablo, Grzech, Anna, Oh, Hyunchul, de Respinis, Moreno, Trzesniewski, Bartek Jacek, Kapteijn, Freek, van de Krol, Roel, Geerlings, Hans, Gascon, Jorge, Hirscher, Michael and Dam, Bernard (2014) Interplay of Linker Functionalization and Hydrogen Adsorption in the Metal–Organic Framework MIL-101. London: Greenwich Academic Literature Archive.
Available at: <http://gala.gre.ac.uk/14410/>

Contact: gala@gre.ac.uk

Interplay of Linker Functionalization and Hydrogen Adsorption in the Metal-Organic Framework MIL- 101

Petra Á. Szilágyi, Ingrid Weinrauch, Jana Juan-Alcañiz, Pablo Serra-Crespo, Anna Grzech, Hyunchul Oh, Moreno de Respinis, Bartek J. Trzeźniewski, Freek Kapteijn, Roesl van de Krol, Hans Geerlings, Jorge Gascon, Michael Hirscher and Bernard Dam*

Dr Petra Ágota Szilágyi

Department of Imaging and Applied Physics, Curtin University, GPO Box U 1987, Perth, WA
6845, Australia

E-mail: Petra.Szilagyi@curtin.edu.au

Ingrid Weinrauch, Hyunchul Oh and Dr Michael Hirscher

Max-Planck-Institut für Metallforschung, Heisenbergstrasse 3, D-70569 Stuttgart, Germany

Dr Jana Juan-Alcañiz, Pablo Serra-Crespo, Moreno de Respinis, Bartek Jacek Trzeźniewski, Prof
Freek Kapteijn, Prof Hans Geerlings, Dr Jorge Gascon and Prof Bernard Dam

Department of Chemical Engineering, Delft University of Technology, Julianalaan 136, 2628
BL, Delft, The Netherlands

Dr Anna Grzech

Civil Engineering and Geosciences, Delft University of Technology, Stevinweg 1, 2628 CN,
Delft, The Netherlands

Dr Roel van de Krol

Helmholtz-Zentrum Berlin für Materialien und Energie, Institute for Solar Fuels, Hahn-Meitner-
Platz 1, 14109 Berlin, Germany

Prof Hans Geerlings

Shell Technology Centre, Grasweg 31, 1031 HW Amsterdam, The Netherlands

ABSTRACT

Functionalization of metal-organic frameworks results in higher hydrogen uptakes owing to stronger hydrogen-host interactions. However, it has not been studied whether a given functional group acts on existing adsorption sites (linker or metal) or introduces new ones. In this work, the effect of two types of functional groups on MIL-101 (Cr) is analyzed. Thermal-desorption spectroscopy reveals that the –Br ligand increases the secondary building unit’s hydrogen affinity, while the –NH₂ functional group introduces new hydrogen adsorption sites. In addition, a subsequent introduction of –Br and –NH₂ ligands on the linker results in the highest hydrogen-store interaction energy on the cationic nodes. The latter is attributed to a *push-and-pull* effect of the linkers.

KEYWORDS: Metal-Organic Frameworks, Post-Synthetic Modification, Hydrogen-Host Interactions, Thermal Desorption Spectroscopy, Debye Force

INTRODUCTION

The urgent need for strategies to reduce our fossil-fuel dependence has spurred many industrialized nations to turn towards alternative sources of energy. The “hydrogen economy”, in which hydrogen is used as a “green” feedstock in fuel cells to power motor vehicles, homes, *etc.* has been highlighted as a potential solution to the energy problem. Challenges to be faced before this becomes a reality include the development of sustainable and fossil-free methods of hydrogen production, the safe and reversible storage and transport of hydrogen, development of affordable hydrogen fuel cell, as well as the development of efficient and reliable hydrogen sensors.¹

Among these issues hydrogen storage is arguably the biggest challenge. While different types of materials are being explored as hydrogen carriers, porous materials have the advantage of offering fast kinetics for hydrogen sorption as well as reversibility over multiple cycles. Among them, metal-organic frameworks (MOFs) are considered as promising materials for non-dissociative hydrogen adsorption. They are organic-inorganic hybrid materials displaying high crystallinity as well as high and regular porosity. In addition, their syntheses can be carried out under mild conditions, allowing for their rational design and facile pre- and post-synthetic modification.²

While some MOFs display extraordinary high hydrogen uptake at cryogenic temperatures, as a result of the generally low enthalpy of hydrogen adsorption (*ca.* 2-8 kJ mol⁻¹)²⁻⁴ being considerably lower than the ideal adsorption enthalpy allowing for ambient-temperature hydrogen storage, 15-25 kJ mol⁻¹,^{5,6} their hydrogen capacity is practically negligible near ambient conditions; a serious drawback for application. Several ways have been identified

leading to enhanced hydrogen-storage capacities in metal-organic frameworks, *via* two major mechanisms: *i*) increase of the surface area or *ii*) increase of the isosteric heat of adsorption. It has been shown through calculations and experimental results that a qualitative linear relationship exists between the H₂ storage capacities and the specific surface areas.^{7,8} However, this relation is only valid at high hydrogen loading, *i.e.* at low temperatures and high pressures.

On the other hand, it has been shown that chemical functionalization of MOFs, *i.e.* the chemical modification of their building blocks, can lead to increased ambient-temperature hydrogen uptake⁹ and to higher enthalpies of hydrogen adsorption. This can take place by two major mechanisms: *i*) by the introduction of additional adsorption sites (on the functional groups), or *ii*) by the secondary effect of the functionalities on the frameworks' polarity, *cf.* by increasing the secondary building unit's hydrogen affinity. This latter phenomenon can be aided by the fact that adsorption of hydrogen on porous materials is driven by the van der Waals interaction or by the Debye force (between a permanent dipole and an induced dipole in the hydrogen molecule). Addition of polar functional groups in the linkers strengthens the Debye force, regardless whether the hydrogen molecule interacts with the positive or the negative part of the dipole. Since MOF linkers are aromatic organics, the addition of functional groups will not only yield stronger dipoles on the functional group but it will also polarize the whole linker and the linker-secondary building unit (SBU, or metal node) bond. Such phenomenon has been shown to remarkably affect catalytic activity of the extremely stable UiO-66, owing to the electronic modulation of the active site by functionalization.¹⁰ Similarly, the impact of the polarization of the linker-secondary building unit through linker functionalization on the photocatalytic activity of isoreticular MOFs has also been recently reported.¹¹

Despite the obvious interest and research efforts, the mechanism of how linker functionalization affects the hydrogen-framework interaction has never been studied directly. In particular, there is a desperate lack of information whether a given functional group acts on existing adsorption sites (linker or metal) or introduces new ones.

In this work, we analyze the effect of two types of functional groups on MIL-101(Cr). MIL-101(Cr) ($\text{Cr}_3\text{FO}[\text{BDC}]_3$, BDC=1,4-benzenedicarboxylate). MIL-101(Cr) has been chosen as starting material owing to its high surface area, its high hydrogen uptake at 77 K and outstanding chemical stability.¹² Although MIL-101 has been suggested not to be a possible starting material for solvent-assisted linker exchange (SALE),¹³ we have recently shown that post-synthetic cation exchange is possible in the same material,¹⁴ suggesting that post-synthetic linker exchange may also be possible. 2-Br-BDC and 2-NH₂-BDC (for molecular structures, see Supporting Information, Figure S1) were chosen as substitute linkers for their highly electronegative functional groups that may allow for different types of interactions with the adsorbent hydrogen molecules: while the –Br functionality is highly polarizable and can thus partake in strong van der Waals interactions, the –NH₂ functionality may allow for more specific interactions through its lone electron pair or *via* dihydrogen bonding. In addition, de Vos and colleagues showed that the –Br and –NH₂ functional groups change the Lewis acidity of the metal corner in the opposite way, whereas –Br ligands increase Lewis acidity, –NH₂ groups were found to decrease it due to electronic effects on the terephthalate linker.¹⁰ Although of all functional groups they studied, the –NO₂ and –NH₂ groups showed the greatest difference in their impact on the metal corner, we opted for the Br functionality as its higher electron density yields larger differences upon

characterization with X-ray based techniques. * Furthermore, Yaghi and co-workers have recently shown that some MOF-5 analogs, synthesized from a mixture of linkers (the so-called multivariate, MTV, MOFs) display enhanced gas uptake when compared with the analogs containing a single type of linkers.¹⁶ Although, the origin of the phenomenon was not discussed, it is possible that the electronic modulation of the metal sites by a partial linker exchange may play a key role in this phenomenon. Therefore, the effect of partial functionalization of MIL-101(Cr) with 2-Br-BDC and 2-NH₂-BDC on the electronic modulation and on the types of hydrogen adsorption sites is also discussed.

MATERIALS AND METHODS

Synthetic Methods: MIL-101(Cr) and Br-MIL-101(Cr) were prepared by direct hydrothermal synthesis, mixing chromium(III) nitrate Cr(NO₃)₃·9H₂O, hydrofluoric acid with 1,4-benzenedicarboxylic acid and by 2-bromo-1,4-benzenedicarboxylic acid, respectively, according to Férey's method.¹⁷ Synthesis of NH₂-MIL-101(Cr) was carried out by the chemical reduction of NO₂-MIL-101(Cr). First, NO₂-MIL-101(Cr) was synthesized similarly to MIL-101(Cr), by replacing H₂BDC by 2-nitro-1,4-benzenedicarboxylic acid. Subsequently, NO₂-MIL-101(Cr) was reduced to NH₂-MIL-101(Cr) by chemical reduction using SnCl₂, according to Stock and co-workers' method,¹⁸ with the only difference being that slightly longer reaction time (16 h) was allowed.

* In addition, NH₂-MIL-101(Cr) cannot be prepared by direct synthetic methods without seriously compromising its crystallinity¹⁵ and is therefore obtained by the reduction of NO₂-MIL-101(Cr) (see Experimental), this results in some unconverted –NO₂ remaining in the framework, which would bias the distinction between the different effects.

Linker Exchange: Linker exchange was carried out as follows: 150 mg MIL-101(Cr) was refluxed for 3 hours with 30 mg 2-bromo-1,4-benzenedicarboxylic acid or 25 mg 2-amino-1,4-benzenedicarboxylic acid in 150 cm³ de-ionized water at 100 °C. In addition, 150 mg previously post-synthetically linker exchanged, Br-BDC-containing, MIL-101(Cr) (**BrPSM**) was refluxed for 3 hours with 25 mg 2-amino-1,4-benzenedicarboxylic acid in 150 cm³ de-ionized water at 100 °C.

Activation of samples: All MOF samples were activated for 6 hours *in vacuo*, at 160 °C following water-to-tetrahydrofuran solvent exchange.

Diffuse Reflectance Infra-Red Fourier Transform (DRIFTS): Spectra were recorded on a Nicolet model 8700 spectrometer, equipped with a high-temperature cell, and a DTGS-TEC detector. The spectra were acquired with 256 scans at 4 cm⁻¹ resolution from 4000 to 500 cm⁻¹ using potassium bromide (KBr) to perform background experiments. The samples were pre-treated at 453 K for 1 hour in a helium flow of 20 cm³ min⁻¹.

UV-Vis diffuse reflectance spectroscopy: Spectra were measured with a Perkin–Elmer Lambda 900 spectrophotometer equipped with an integrating sphere (“Labsphere”) in the 200–800 nm range. Kubelka–Munk function was used to convert reflectance measurements into equivalent absorption spectra using the reflectance of BaSO₄ as reference.

Determination of the extent of linker substitution: The extent of post-synthetic linker exchange was determined by area integral of *i*) the UV-Vis spectra: MIL-101(Cr) spectrum was used as background subtraction, and the curve was integrated over a maximum at 380 nm, between 307 and 475 nm as well as of that of *ii*) the DRIFT spectra: a linear baseline was used as background for the integration of symmetric and asymmetric $\nu(-\text{NH}_2)$ between 3317-3545 cm⁻¹, with

maximum peaks around 3370 and 3520 cm^{-1} respectively. In case of the Br-BDC containing samples, the sum of the normalized and baseline-corrected ortho- and meta-substituted Ar-Br stretch combination modes (at 1042 and 1072 cm^{-1} , respectively) was used to determine the extent of the linker exchange.

Nuclear Magnetic Resonance Spectroscopy: Because of the highly paramagnetic Cr^{3+} ions, a customized digestion method was applied for the SALE-modified samples; the samples were digested in an aqueous H_2O_2 solution, which also allowed for the oxidation of the Cr^{3+} ions. The solvent was subsequently evaporated and the organic part of the remaining powder was dissolved in deuterated DMF. Proton NMR spectra were recorded on the digested samples using a Bruker Avance-400 spectrometer. We would like to note that due to the complexity of the digestion method (hindered by the necessity of control oxidation states, linker solubility and signal multiplicity issues) and the consequent uncertainty of the preservation of linker ratios we only used the NMR spectra to demonstrate the presence of various linkers.

Scanning Electron Microscopy: Shape, size and morphology of all samples were investigated by SEM (JSM-7500F) using an electron beam energy of 5 keV.

Synchrotron X-ray Powder diffraction and analysis: Diffraction data was collected on beamline ID31 at the European Synchrotron Radiation Facility using a monochromatic X-ray beam of $\lambda=0.4305 \text{ \AA}$. Each sample was activated prior to data collection and subsequently loaded into capillaries in an Ar glove box. The capillary was being spun throughout the SXRPD data collection, which was detected using a series of 9 multi-analyzing Si (1 1 1) crystal-detectors.¹⁹ Cell parameters of the samples were determined in the $Fd\bar{3}m$ space group, as found by Férey and colleagues for the pristine MIL-101(Cr),¹⁷ using the LeBail refinement mode as implemented in

the GSAS analytical software package.²⁰ Due to the low-angle asymmetry, lattice parameters and Gaussian line shapes were determined from the higher angle region (1.5-3 deg) and subsequent peak-shape fitting was carried out on the whole pattern, leaving the lattice parameters and Gaussian line terms unaltered. Powder patterns of Br-MIL-101(Cr) and NH₂-MIL-101(Cr) were simulated as follows: the crystallographic information file of pristine MIL-101(Cr)¹⁷ was loaded in Wincrystals 2000²¹ and missing hydrogen atoms were placed on the linkers' aromatic rings and a new crystallographic information file was generated thereof, the hydrogen atoms on the aromatic linkers were then exchanged to Br and N, respectively, their multiplicity was decreased to ¼, and the final crystallographic information files were thus generated, which were then used to simulate their powder pattern at $\lambda=0.4305 \text{ \AA}$.

Determination of the Brunauer-Emmett-Teller (BET) surface area: N₂ adsorption of the activated samples was carried out using an Autosorb 6B-type nitrogen-adsorption instrument at 77 K. The isotherms obtained were then fitted using the BET function, as implemented in the instrument's software package.

Hydrogen adsorption: Hydrogen adsorption and desorption isotherms were recorded at 298 and 77 K, in a Sievert's apparatus (HyEnergy, PCTPro-2000) up to *ca.* 30 bar hydrogen pressure. Due to their sensitivity towards moisture, the activated samples were loaded into the microdoser in a glove box, under Ar atmosphere.

High-resolution, low-temperature hydrogen-sorption isotherms of MOF samples at 19.5 K were measured with laboratory-designed volumetric adsorption equipment with a temperature controlled cryostat. Around 23 mg of MOF samples were activated under ultra-high vacuum at 150 °C overnight, prior to each measurement. For the laboratory-designed cryostat, the

temperature control was calibrated by measuring the liquefaction pressure for hydrogen and nitrogen in the empty sample chamber at various temperatures.

Thermal Desorption Spectroscopy (TDS): TDS spectra of H₂ and D₂ were acquired using the setup described in reference 22 as follows: prior to the measurement 2-4 mg sample was heated at 470 K in high vacuum (below 10⁻⁵ mbar) for approximately 3 h to remove moisture and adsorbed gases. Then the sample was slowly cooled down to approximately 20 K, and was loaded with 10 mbar of hydrogen or deuterium, after the addition of the gas, the sample was kept under pressure for 5 min at 20 K. Subsequently, the reactor was evacuated for several minutes (final pressure was below 10⁻⁷ mbar) to remove the non-adsorbed hydrogen (or deuterium) molecules. Owing to the low temperature of the sample, adsorbed H₂ and D₂ stick to the surface of the adsorbent even under vacuum, while the free molecules can be easily pumped off. Then the temperature program was started with a constant heating rate of 0.1 K s⁻¹ and the signal of desorbed hydrogen, deuterium and HD molecules was recorded with the mass spectrometer. In addition, the masses 1 and 18 of atomic hydrogen and water, respectively, were measured. Desorption spectra were recorded up to 160 K.[†]

Integration of the desorption peaks was performed by the subtraction of base line defined from the high-temperature range (above 150 K) of the spectra, subsequently Gaussian peak shapes were fitted whose area is proportional to the number of gas molecules desorbed and can be quantified after calibration.

[†] Several spectra were acquired up to 300 K, and as no hydrogen desorption occurred above 160 K, the rest of the spectra were only acquired up to 160 K.

Thermo-Gravimetric Analysis (TGA): Thermal analysis of the materials (Supporting Information, Figure S9) was carried out using a system provided by Mettler Toledo, model TGA/SDTA851e. First the samples were treated under air flow at 323 K to eliminate moisture for one hour and then analyzed under air flow of $60 \text{ cm}^3 \text{ min}^{-1}$ at a temperature rate of 5 K min^{-1} .

RESULTS AND DISCUSSION

In order to investigate the mechanism of the effect of linker functionalization on the hydrogen-framework interaction, MIL-101(Cr)¹⁷ and NH₂-MIL-101(Cr)¹⁸ have been synthesized according to the literature, Br-MIL-101(Cr) has been synthesized analogously to MIL-101(Cr). In addition, solvent-assisted linker exchange was applied to obtain post-synthetically modified (PSM), partially linker exchanged **BrPSM** (2-Br-BDC substituted MIL-101(Cr)), **NH₂PSM** (2-NH₂-BDC substituted MIL-101(Cr)) and **BrNH₂PSM** (2-NH₂-BDC and 2-Br-BDC substituted MIL-101(Cr)). We have identified successful linker exchange, as demonstrated by UV-Vis (Supporting Information, Figure S2), DRIFT (Supporting Information, Figure S3) and ¹H NMR spectroscopy (see Experimental and Supporting Information, Figure S1). From this data the extent of the linker exchange could be determined, which amounts to *ca.* 20 % of all linkers (Supporting Information, Table S1).

First, the samples' hydrogen-storage properties were probed by equilibrium adsorption experiments at 77 and 298 K. Figure 1 shows the adsorption isotherms of the MTV and pristine (containing only one kind of linker) MOFs. At 77 K, the pristine MIL-101(Cr) shows the highest hydrogen uptake, in good agreement with the N₂ physisorption measurements at the same temperature (Supporting Information, Table S2). In other words, the saturation hydrogen uptake (the concentration beyond which hydrogen uptake does not increase further with increasing

hydrogen pressure) was found to be governed by the available surface area (MIL-101 – 2136 m² g⁻¹, Br-MIL-101 – 840.6 m² g⁻¹, NH₂-MIL-101 – 2001 m² g⁻¹, **BrPSM** – 1940 m² g⁻¹, **NH₂PSM** – 2059 m² g⁻¹ and **BrNH₂PSM** – 1839 m² g⁻¹), as displayed in the low temperature hydrogen isotherm (Figure 1a). In contrast, at ambient temperature and at much lower hydrogen loadings, the hydrogen uptake of samples **BrPSM**, **NH₂PSM** and **BrNH₂PSM** is 20-40% higher than that of MIL-101(Cr). In addition, NH₂-MIL-101(Cr) also showed relatively high hydrogen-adsorption capacity at room temperature, while Br-MIL-101(Cr) shows again the lowest hydrogen uptake. In addition, hydrogen uptake per formula unit was observed to increase compared to that of MIL-101(Cr) (0.393 mole H₂) by 50% for **BrNH₂PSM** (0.573 mole H₂) under 25 bar hydrogen pressure at 298 K. **BrPSM** (0.471 mole H₂), **NH₂PSM** (0.524 mole H₂) and NH₂-MIL-101(Cr) (0.446 mole H₂) also showed increased hydrogen uptake per formula unit, while Br-MIL-101(Cr) (0.207 mole H₂) showed poorer performance at 298 K.

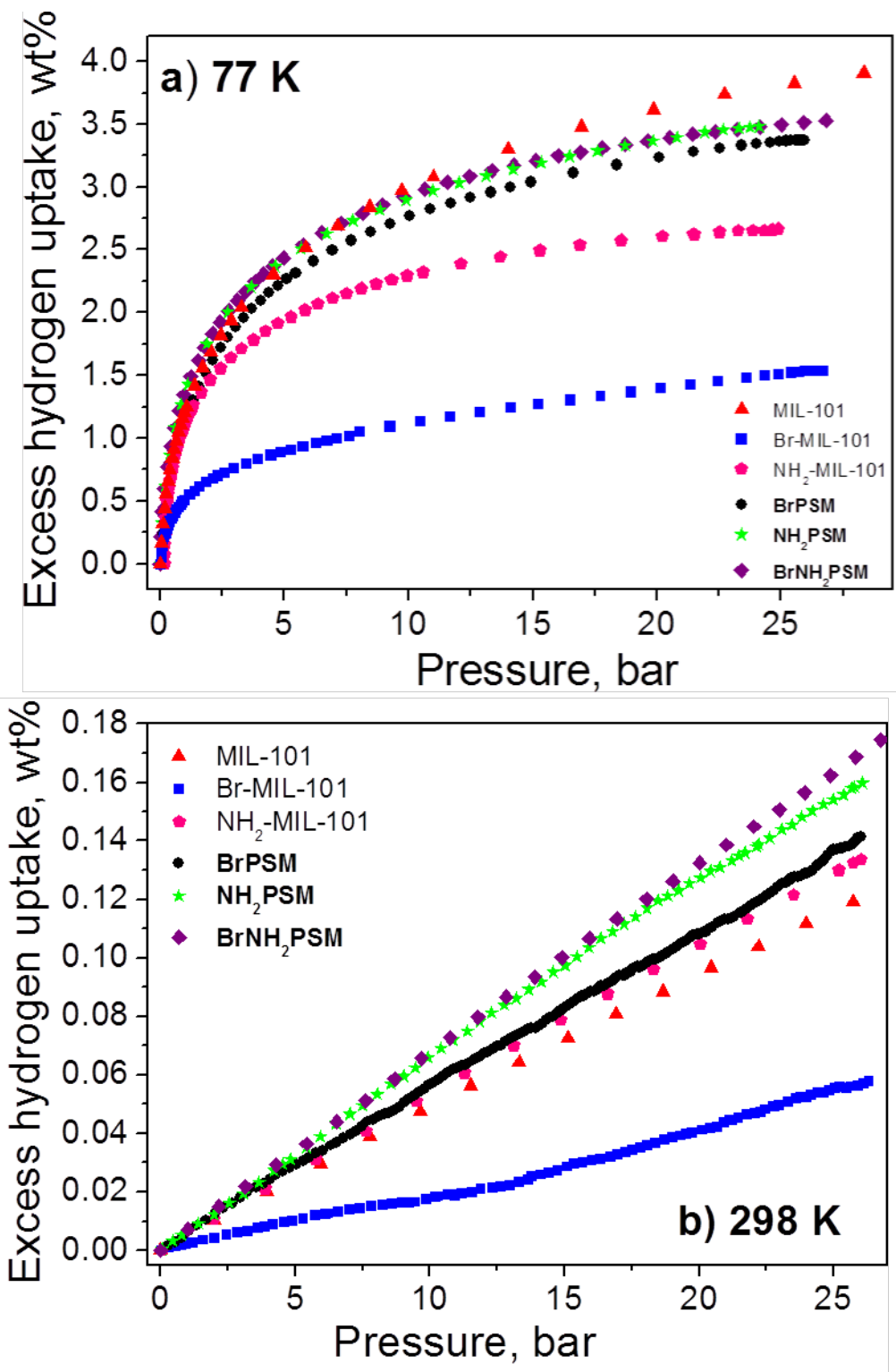


Figure 1 H₂-sorption isotherms of MIL-101(Cr), Br-MIL-101(Cr), NH₂-MIL-101(Cr) and samples BrPSM, NH₂PSM and BrNH₂PSM at **a)** 77 K and **b)** 298 K

If the impact of linkers on the amount and nature of hydrogen adsorption sites is to be investigated, a number of other effects that may also result in increased hydrogen uptake need to be safely excluded. Trivial reasons such as a phase transition can be dismissed on the basis of our powder X-ray diffraction results (Supporting Information, Figure S4), this may be relevant as MIL-101(Cr) is known to be the thermodynamically disfavored Cr(BDC) polymorph (as opposed to MIL-53).²³

Powder X-ray diffraction data (PXRD) was collected on all samples and it was possible to index all patterns in the $Fd\bar{3}m$ space group (Supporting Information, Table S3), which confirms that the hydrogen-uptake enhancement upon SALE is not due to structural changes. It has been shown that the formation of core-shell particles may be indicated as two phases in the diffractogram in case the particles are large enough.²⁴ On the other hand, when the shell of core-shell crystallites are too thin to diffract individually, broadening of the diffraction peaks of the core would be observed, since the same batch of MIL-101(Cr) was used for the solvent-assisted linker exchange and powder X-ray diffraction data collection. The reason for such a line broadening would be the following: while the crystallite size of the starting and post-synthetically modified samples remains the same (for SEM images see Supporting Information, Figure S6), the particles would be built up of two sub-structures (core and shell), with different lattice parameters (as determined from the powder pattern of the pure MIL-101(Cr), Br-MIL-101(Cr) and NH₂-MIL-101(Cr)). The particle sizes observed in the PXRD pattern would thus appear to be smaller, which, in turn, would result in line broadening. We have observed that the pattern in each diffractogram displays one phase only. In addition, the peak-shape analysis of the diffraction pattern shows that the obtained crystallites are comparable in size with the initial

ones. It can be thus safely concluded that the post-synthetic linker exchange took place randomly throughout the particles' pore space.

In addition, pore narrowing in the case of NH₂-MIL-101(Cr) can also play some role, which might be a consequence of its indirect preparation.^{18,25} The reaction pathway for the indirect preparation route does not allow for the complete removal of the reactant from the pores to a small extent, which in turn may modify the material's hydrogen uptake.²⁶ In contrast, further analysis of the diffraction data reveals that pore narrowing can be excluded as the reason of the increase of the hydrogen uptake in the post-synthetically modified samples. The (0 2 2):(1 1 3) diffraction-peak ratio has been highlighted as a sensitive measure of pore filling.²⁷ On the other hand, our simulations show that linker substitution does not have a large impact on the above diffraction-peak ratio and indeed we have not observed any substantial change upon post-synthetic linker exchange (Supporting Information, Figure S5), confirming that the increase of the hydrogen uptake is due to linker substitution and not to pore narrowing.

In case of the framework's electronic modulation by linker exchange, the Debye forces of the framework-hydrogen interaction should change significantly, in particular on the modulated sites of the framework such as the metal nodes or the linker functionalities. As these latter ones may also act as added adsorption sites, the host-hydrogen interactions would be further modified. Attention needs to be drawn to the differences in the enthalpies of adsorption of hydrogen on the various sites of the frameworks: for example, it has been shown that hydrogen has a stronger interaction with the metal unit than with the aromatic ring.²⁸ In order to probe the effect of linker-exchange on the strength of Debye interactions between the framework and the hydrogen molecules, the enthalpy of hydrogen adsorption has been determined at hydrogen loading of 0.2 wt% (Table 1), close to the maximum uptake at ambient temperature. Our results show a very

slight increase of the adsorption enthalpy at relatively low (0.2 wt%) hydrogen loading, when compared with the pristine MIL-101(Cr).

Table 1. Comparison of hydrogen adsorption enthalpies for MIL-101(Cr), Br-MIL-101(Cr), NH₂-MIL-101(Cr) and samples **BrPSM**, **NH₂PSM** and **BrNH₂PSM** at 0.2 wt% loading.

Material	MIL-101[a]	Br-MIL-101	NH ₂ -MIL-101	BrPSM	NH₂PSM	BrNH₂PSM
ΔH_{ads} , kJ mol ⁻¹	4.23(1)	4.10(2)	4.31(2)	4.27(4)	4.28(4)	4.32(2)

^[a] Somewhat lower but still in agreement with the literature data.²⁹

It can be thus concluded that linker functionalization increases the ambient-temperature hydrogen uptake of MIL-101(Cr), although the gravimetric hydrogen uptake in this regime for the fully functionalized Br-MIL-101(Cr) was not enhanced due to the large mass of the framework. The increased hydrogen uptake can be attributed to a stronger hydrogen-host interaction, as reflected by the enthalpies of adsorption measured. This is in line with previous observations,^{5,6} however, it does not reveal the underlying physical phenomena. As an example, NH₂-MIL-101(Cr) and **BrPSM** show similar adsorption isotherms at both, 77 and 298 K, in addition, the enthalpies of hydrogen adsorption on them are also a fair match, despite having different functional groups and a different extent of linker functionalization.

In order to reveal the effect of electronic modulation by linker substitution and of those of the linker functional groups as adsorption sites, the hydrogen-framework interactions need to be analyzed in detail. Thermal desorption spectroscopy has been highlighted as an unrivalled tool to get insight into the strength of hydrogen-host interactions.^{22,29,30} Desorption of hydrogen as a function of temperature from all samples was therefore monitored.

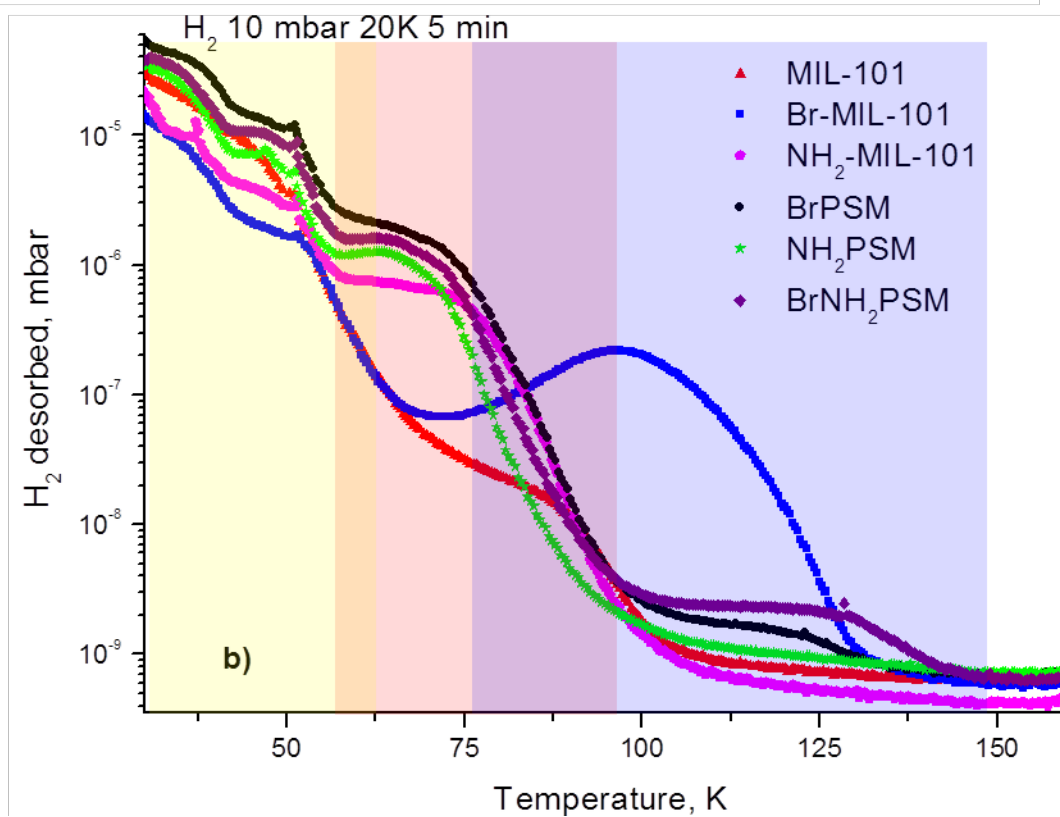
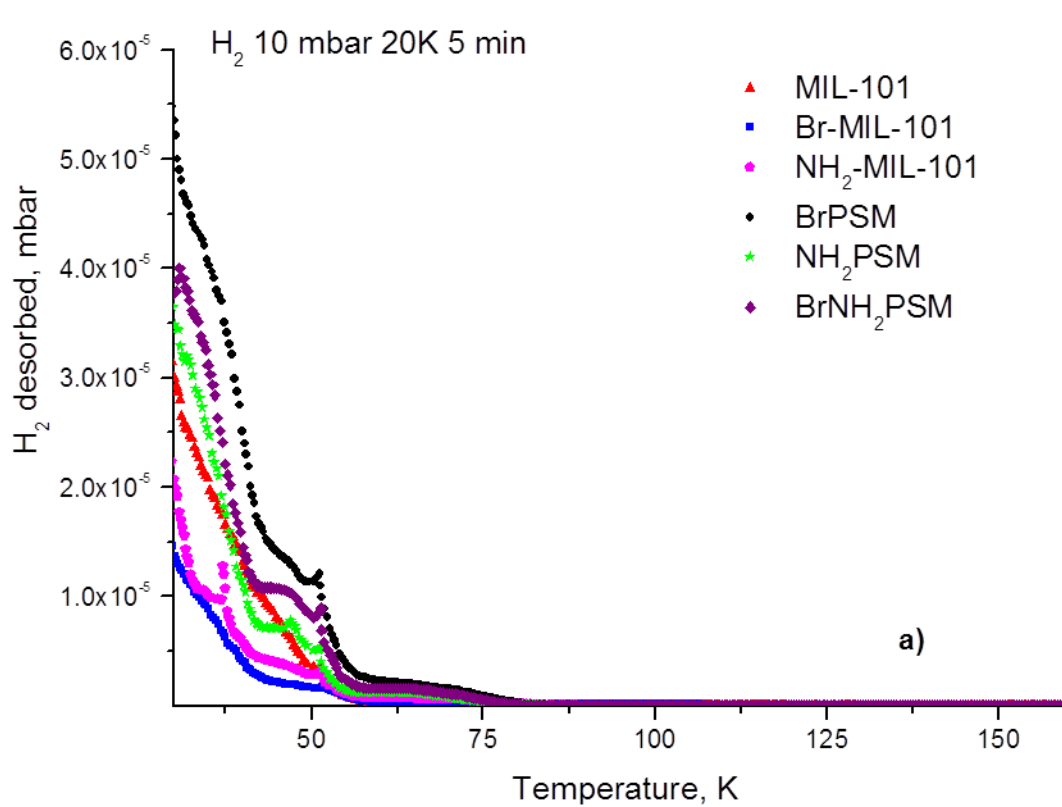


Figure 2 TDS spectra of hydrogen from various MOFs shown **a)** on linear and **b)** semi-logarithmic scale, showing the three different desorption regions: *in yellow*: desorption from the pores and linkers, *in pink*: desorption from the functional groups of the linkers and *in blue*; desorption from the SBU. Note that the range of the three different regions varies somewhat for different linkers, whence the intermediate regions (orange and purple).

Note that the sharp peaks at *ca.* 25 and 50 K are artifacts; they are a consequence of the change of PID parameters.

In the TDS spectra, various desorption ranges corresponding to different adsorption sites are clearly discernible and can be divided into three regions (Figure 2). The lowest temperature region (up to *ca.* 40 K) can be described as the convolution of the desorption signals from the weakest adsorption sites, aromatic rings for instance, and the boiling of the liquid hydrogen trapped in the pores.

Between *ca.* 40 K and 70 K desorption off the linkers is displayed in the spectra (Figure 2a).

While MIL-101(Cr) and Br-MIL-101(Cr) yield only one desorption peak in this region, the appearance of an additional peak centered between 60 and 70 K can be observed, for the case of NH₂-MIL-101(Cr) (Figure 2b). In addition, this last peak is also present in the spectra of all the amino functional-group containing samples (NH₂PSM and BrNH₂PSM).[‡] This suggests that the introduction of –NH₂ groups in the MOF's framework introduces new adsorption sites.

[‡] As this is the only additional peak in the TDS spectrum of NH₂-MIL-101(Cr), it is possible to exclude that the increased hydrogen uptake may be a consequence of pore narrowing by the remaining SnCl₂. The reason for this being that this peak is identical to those found on the post-synthetically functionalized –NH₂-containing NH₂PSM and BrNH₂PSM, which do not contain SnCl₂ in their pores.

On the other hand, fully functionalized Br-MIL-101(Cr) apparently does not have more (or different) hydrogen adsorption sites than the pristine MIL-101(Cr). Partially linker-exchanged **BrPSM**, however, displays similar behavior to the samples containing amino functionalities. One possible explanation for this phenomenon is that, the organic functional group would polarize the whole aromatic linker. If the linkers are substituted in a symmetrical and ordered fashion, some of the polarization would be lost, as the influence of two functionalized linkers may counterbalance each other. Conversely, random linker substitution results in stronger dipole interactions and, therefore, a stronger interaction between H₂ and its adsorption site.

The highest temperature region of the TDS spectra, *i.e.* above 80 K corresponds to hydrogen desorption off the inorganic building unit (Figure 1a). A striking feature of the spectra in this region is that whenever –Br ligands are present, the desorption temperature is shifted to higher temperature values. This reveals that the addition of Br functionalities will polarize the linker-secondary building unit bond; this observation has also been confirmed by our low-temperature hydrogen adsorption data (Supporting Information, Figure S7).

The fact that no such effect has been observed for amino functionalities is in line with the observations of de Vos *et al.* who found that –Br ligands increase Lewis acidity while –NH₂ groups were found to decrease it.⁷ It can be thus assumed in a first instance that, in order to obtain stronger hydrogen-SBU interactions, stronger Lewis acids need to be applied on the cationic nodes. On the other hand, the highest hydrogen desorption temperature has been observed in the case of the **BrNH₂PSM**, this phenomenon can be explained by the two opposite effects of the –NH₂ and –Br functional groups, resulting in a *push-and-pull* force, which in turn further increases the hydrogen affinity of the site.

Desorption of deuterium shows very similar trends to that of hydrogen, confirming that the observed phenomena are only related to desorption of hydrogen from the frameworks (Supporting Information, Figure S8).

Upon integrating the peaks in the TDS spectra, a qualitative analysis of the desorption of hydrogen from the MOFs can be carried out and the results are summarized in Table 2.

Table 2. Analysis of TDS spectra[§]

MOF	Desorption temperature (center, K)	wt%	Desorption site – region	In 298 K isotherm
MIL-101(Cr)	87	10 ⁻⁴	SBU	Yes
	38	0.6	Linker +	Partly
	30	1.1	H ₂ boil off	No
Br-MIL-101(Cr)	96	0.02	SBU	Yes
	46	0.1	Linker +	Yes
	32	0.4	H ₂ boil off	Partly
NH ₂ -MIL-101(Cr)	Up to 75	10 ⁻⁴	SBU	Yes
	64	0.1	Functionality	Yes
	43	0.2	Linker +	Partly
	31	0.4	H ₂ boil off	No
BrPSM	114	10 ⁻⁴	SBU	Yes
	64	0.1	Functionality	Yes
	45	0.6	Linker +	Partly

[§] This analysis also highlights that at 0.2 wt% loading, hydrogen desorbs at higher temperatures (owing to stronger hydrogen-host interactions) in the case of the three post-synthetically modified samples and NH₂-MIL-101(Cr) than in the case of the pristine MIL-101(Cr) and the Br-MIL-101(Cr), in good agreement with the adsorption enthalpies determined.

	34	1.7	H ₂ boil off	No
NH₂PSM	Up to 87	7x10 ⁻⁵	SBU	Yes
	62	0.1	Functionality	Yes
	46	0.5	Linker +	Partly
	33	1.2	H ₂ boil off	No
BrNH₂PSM	118	1.5x10 ⁻⁴	SBU	Yes
	62	0.1	Functionality	Yes
	46	0.5	Linker +	Partly
	31	1.2	H ₂ boil off	No

The three regions mentioned above (highlighted in Fig. 2b) can be now quantified as *i*) convolution of hydrogen liquid boil off from the pores and desorption from the lowest enthalpy adsorption sites takes place in the 30-40 K region; *ii*) hydrogen desorbs from the functional groups in the 40-70 K region and *iii*) from the secondary building unit in the 70-120 K region.**

The opposite effect of the –Br and –NH₂ groups on the Lewis acidity of the secondary building can also be observed upon close inspection of the data in Figure 2. The desorption peak of hydrogen from the SBU of the pristine MIL-101(Cr) is centered at about 87 K, which was increased to 96 K on a total Br-functionalization and did not substantially change for NH₂-MIL-101(Cr), resulting in its desorption peak practically overlapping with that of the functional groups.

** Overlap of the distinct region is due to different temperatures of hydrogen desorption in the different MOFs.

As the materials only adsorb up to *ca.* 0.2 wt% at 298 K under *ca.* 30 bar hydrogen pressure, the TDS spectra explain why NH₂-MIL-101(Cr), **BrPSM**, **NH₂PSM** and **BrNH₂PSM** have the highest uptake under these conditions: at this uptake range (up to 0.2 wt%), the adsorption is governed by the functional groups and their random distribution. As Br-MIL-101(Cr) and MIL-101(Cr) have no functional groups that could adsorb in this region, their hydrogen uptake is consequently lower. Although Br-MIL-101(Cr) displays an increased hydrogen uptake on the SBUs, this phenomenon is of such a low extent in terms of the number of hydrogen molecules adsorbed that it practically has no effect in the ambient-temperature hydrogen isotherm. In fact, ambient-temperature isotherms and the TDS maxima at higher temperatures show *ca.* 0.1 wt%, which corresponds to a lower than 10% occupancy of the available adsorption sites. In addition, the slight increase of the enthalpies of hydrogen adsorption on the post-synthetically modified samples can be also rationalized as the adsorption in the up to 0.2 wt% range is governed by the linkers, including the functional groups. While at this loading the increase of the adsorption enthalpies is below 2.5%, it is anticipated that at zero coverage the difference is substantially larger, as reflected by the *ca.* 40 K higher hydrogen-desorption temperature from the secondary building unit of **BrNH₂PSM** than that of the pristine MIL-101(Cr) (Figure 2b), at the applied 0.1 K s⁻¹ heating rate.

While both functionalities improved hydrogen-framework interactions (the –Br ligand increases the SBU's hydrogen affinity, while the –NH₂ functional group introduces new hydrogen adsorption sites), the introduction of amino groups can be a more viable option for hydrogen-storage applications since the increased hydrogen uptake due to the SBUs' higher hydrogen affinity has only a minor effect (an additional 0.02 wt%, although at relatively high temperatures). Partially linker-exchanged samples have proven to be the best option as they benefit from both

effects, in particular for the MOF containing both types of functional groups, which shows the strongest hydrogen-SBU interaction.

CONCLUSIONS

In the present work the effect of linker substitution on the electronic modulation of the MIL-101(Cr) metal-organic framework has been studied. Particular emphasis was given to the hydrogen-host interactions as a function of the electronic properties of the substituting linkers as well as the extent of linker substitution (total or partial). In order to achieve partial linker exchange, solvent-assisted linker exchange in MIL-101(Cr) was successfully employed and it was found that it results in increased ambient-temperature hydrogen uptake due to stronger hydrogen-host interactions, as reflected in the enthalpies of hydrogen adsorption. Our results suggest that $-\text{Br}$ functionalities act mainly on the metal site and do not form an independent adsorption site (unless only partially introduced into the framework). In contrast, $-\text{NH}_2$ functionalities do not improve the metal-site-hydrogen interaction substantially, but they do form additional adsorption sites. Partial linker exchange did not yield a lot of difference in comparison with the total functionalization when only $-\text{NH}_2$ groups were introduced in MIL-101(Cr), apart from the obvious difference in the molar mass. Subsequent introduction of $-\text{Br}$ and $-\text{NH}_2$ ligands resulted in the highest hydrogen-store interaction energy on the cationic nodes. The latter is attributed to the opposite electronic modulating effect, *push-and-pull*, of the distinct linkers. While these observations highlight the importance of functional groups when addressing hydrogen storage in metal-organic frameworks, the resultant ambient-temperature hydrogen-uptake increase is too small for applications. Furthermore, the knowledge generated on the adsorption mechanism of hydrogen on functionalized MOFs may be beneficial for gas separation and catalytic applications.

ASSOCIATED CONTENT

AUTHOR INFORMATION

Corresponding Author

* Dr Petra Ágota Szilágyi, to whom correspondence should be sent

Department of Imaging and Applied Physics, Curtin University, GPO Box U 1987, Perth, WA
6845, Australia

E-mail: Petra.Szilagyi@curtin.edu.au

Author Contributions

The manuscript was written through contributions of all authors. All authors have given approval to the final version of the manuscript.

Funding Sources

Agenstchap.nl (Energy Innovation Funding Agency), ref nr. EOSLT07052

ACKNOWLEDGMENT

The authors thank the Agenstchap.nl (Energy Innovation Funding Agency) for funding (ref nr. EOSLT07052) and the European Synchrotron Radiation Facility for provision of beamtime. Particular thanks are due to Ruben Abellon, Frans Oostrum and Willy Rook for experimental support.

SUPPORTING INFORMATION AVAILABLE

NMR spectra, UV-Vis spectra, DRIFT spectra with assignments, linker compositions calculated, BET surface areas, SPXRD patterns with Le Bail fits, and lattice parameters determined, SEM

images, low-temperature high-resolution hydrogen adsorption isotherms, D₂ desorption spectra and TGA curves are presented. This material is available free of charge *via* the Internet at <http://pubs.acs.org>.

ABBREVIATIONS

MOF – metal-organic framework; SBU – secondary building unit; BDC – 1,4-benzenedicarboxylic acid; MTV - multivariate; SALE – solvent-assisted linker exchange; PSM – post-synthetic modification; UV-Vis – UV-visible; DRIFT – diffuse reflectance infra-red; NMR – nuclear magnetic resonance; PXRD – powder X-ray diffraction; SPXRD – synchrotron powder X-ray diffraction; SEM – scanning electron microscopy; TDS – thermal desorption spectroscopy; PID - photoionization detector; BET – Brunauer–Emmett–Teller

REFERENCES

- [1] Tollefson, J., Hydrogen Vehicles: Fuel of the Future? *Nature*, **2010**, 1262-1264
- [2] Sculley, J.; Yuan, D., and Zhou, H.-C., The Current Status of Hydrogen Storage in Metal–Organic Frameworks—Updated. *Energy Environ. Sci.*, **2011**, 4, 2721-2735
- [3] Murray, L. J.; Dincă, M., and Long, J. R., Hydrogen Storage in Metal–Organic Frameworks. *Chem. Soc. Rev.*, **2009**, 38, 1294-1314
- [4] Zhao, D.; Yuan, D., and Zhou, H. C., The Current Status of Hydrogen Storage in Metal–Organic Frameworks. *Energy Environ. Sci.*, **2008**, 1, 222-235
- [5] Bhatia, S. K. and Myers, A. L., Optimum Conditions for Adsorptive Storage, *Langmuir*, **2006**, 22, 1688-1700

- [6] Bae, Y.-S., and Snurr, R. Q., Optimal Isothermic Heat of Adsorption for Hydrogen Storage and Delivery Using Metal–Organic Frameworks. *Micropor. Mesopor. Mater.*, **2010**, *132*, 300-303
- [7] Wong-Foy, A. G.; Matzger, A. J., and Yaghi, O. M., Exceptional H₂ Saturation Uptake in Microporous Metal–Organic Frameworks. *J. Am. Chem. Soc.*, **2006**, *128*, 3494-3495
- [8] Panella, B.; Hirscher, M.; Pütter H., and Müller, U., Hydrogen Adsorption in Metal–Organic Frameworks: Cu-MOFs and Zn-MOFs Compared. *Adv. Funct. Mater.*, **2006**, *16*, 520-524
- [9] Rowsell, J. L. and Yaghi, O. M., Effects of Functionalization, Catenation, and Variation of the Metal Oxide and Organic Linking Units on the Low-Pressure Hydrogen Adsorption Properties of Metal–Organic Frameworks. *J. Am. Chem. Soc.*, **2006**, *128*, 1304-1315
- [10] Vermoortele, F.; Vandichel, M.; van de Voorde, B.; Ameloot, R.; Waroquier, M.; van Speybroeck, V., and de Vos, D. E., Electronic Effects of Linker Substitution on Lewis Acid Catalysis with Metal–Organic Frameworks. *Angew. Chem. Int. Ed.*, **2012**, *51*, 4887-4890
- [11] Gascon, J.; Hernández-Alonso, M. D.; Almeida, A. R.; van Klink, G. P. M.; Kapteijn, F., and Mul, G., Isorecticular MOFs as Efficient Photocatalysts with Tunable Band Gap: An Operando FTIR Study of the Photoinduced Oxidation of Propylene. *ChemSusChem*, **2008**, *1*, 981-983
- [12] Latroche, M.; Surblé, S.; Serre, C.; Mellot-Draznieks, C.; Llewellyn, P. L.; Lee, J.-H.; Chang, J.-S.; Jung, S. H., and Férey, G., Hydrogen Storage in the Giant-Pore Metal–Organic Frameworks MIL-100 and MIL-101 *Angew. Chem. Int. Ed.*, **2006**, *45*, 8227-8231

- [13] Kim, M.; Cahill, J. F.; Fei, H.; Prather, K. A., and Cohen, Postsynthetic Ligand and Cation Exchange in Robust Metal–Organic Frameworks. S. M., *J. Am. Chem. Soc.*, **2012**, *134*, 18082-18088
- [14] Szilágyi, P. Á.; Serra-Crespo, P.; Dugulan, I.; Gascon, J.; Geerlings, H., and Dam, B., Post-Synthetic Cation Exchange in the Robust Metal–Organic Framework MIL-101(Cr). *Cryst. Eng. Comm.*, **2013**, *15*, 10175-10178
- [15] Jiang, D.; Keenan, L. L.; Burrows, A. D., and Edler, K. J., Synthesis and Post-Synthetic Modification of MIL-101(Cr)-NH₂ via a Tandem Diazotisation Process. *Chem. Commun.*, **2012**, *48*, 12053-12055
- [16] Deng, H.; Doonan, C. J.; Furukawa, H.; Ferreira, R. B.; Towne, J.; Knobler, C. B.; Wang, B., and Yaghi, O. M., Multiple Functional Groups of Varying Ratios in Metal-Organic Frameworks. *Science*, **2010**, *327*, 846-850
- [17] Férey, G.; Mellot-Draznieks, C.; Serre, C.; Millange, F.; Dutour, J.; Surblé S., and Margiolaki, I., A Chromium Terephthalate-Based Solid with Unusually Large Pore Volumes and Surface Area. *Science*, **2005**, *309*, 2040-2042
- [18] Bernt, S.; Guillerm, V.; Serre C., and Stock, N., Direct Covalent Post-Synthetic Chemical Modification of Cr-MIL-101 Using Nitrating Acid. *Chem. Commun.*, **2011**, *47*, 2838-2840
- [19] Hodeau, J.-L. ; Bordet, P. ; Anne, M.; Prat, A.; Fitch, A. N.; Dooryhee, E.; Vaughan, G., and Freund, A. K., Nine-Crystal Multianalyzer Stage for High-Resolution Powder Diffraction between 6 keV and 40 keV. *Proc. SPIE*, **1998**, *3448*, 353-361

- [20] Larson, A. C. and von Dreele, R. B., General Structure Analysis System (GSAS); Los Alamos National Laboratory: Los Alamos, NM, **1994**
- [21] Betteridge, P. W.; Carruthers, J. R.; Cooper, R. I.; Prout, K., and Watkin, D. J., CRYSTALS Version 12: Software for Guided Crystal Structure Analysis. *J. Appl. Cryst.*, **2003**, *36*, 1487
- [22] Panella, B.; Hirscher, M., and Ludescher, B., Low-Temperature Thermal-Desorption Mass Spectroscopy Applied to Investigate the Hydrogen Adsorption on Porous Materials. *Micropor. Mesopor. Mat.*, **2007**, *103*, 230-234
- [23] Bauer, S.; Serre, C.; Devic, T.; Horcajada, P.; Marrot, J.; Férey, G., and Stock, N., High-Throughput Assisted Rationalization of the Formation of Metal Organic Frameworks in the Iron(III) Aminoterephthalate Solvothermal System. *Inorg. Chem.*, **2008**, *47*, 7568-7576
- [24] Szilágyi, P. Á.; Lutz, M.; Gascon, J.; Juan-Alcañiz, J.; van Esch, J.; Kapteijn, F.; Geerlings, H.; Dam, B., and Van De Krol, R., MOF@MOF Core–Shell vs. Janus Particles and the Effect of Strain: Potential for Guest Sorption, Separation and Sequestration. *Cryst. Eng. Comm.*, **2013**, *15*, 6003-6008
- [25] Lin, Y.; Kong, C., and Chen, L., Direct Synthesis of Amine-Functionalized MIL-101(Cr) Nanoparticles and Application for CO₂ Capture. *RSC Adv.*, **2012**, *2*, 6417-6419
- [26] Botas, J. A.; Calleja, G.; Sánchez- Sánchez, M., and Orcajo, M. G., Cobalt Doping of the MOF-5 Framework and Its Effect on Gas-Adsorption Properties. *Langmuir*, **2010**, *26*, 5300-5303

- [27] Hu, X.; Lu, Y.; Dai, F.; Liu, C., and Liu, Y., Host–Guest Synthesis and Encapsulation of Phosphotungstic Acid in MIL-101 *via* “Bottle around Ship”: An Effective Catalyst for Oxidative Desulfurization. *Micropor. Mesopor. Mat.*, **2013**, *170*, 36-44
- [28] Turnes Palomino, G., Palomino Cabello, C., and Otero Areán, C., Enthalpy–Entropy Correlation for Hydrogen Adsorption on MOFs: Variable-Temperature FTIR Study of Hydrogen Adsorption on MIL-100(Cr) and MIL-101(Cr). *Eur. J. Inorg. Chem.*, **2011**, *11*, 1703-1708
- [29] Dybtsev, D.; Serre, C.; Schmitz, B.; Panella, B.; Hirscher, M.; Latroche, M.; Llewellyn, P. L.; Cordie, S.; Molard, Y.; Haouas, M. *et al.*, Influence of $[\text{Mo}_6\text{Br}_8\text{F}_6]^{2-}$ Cluster Unit Inclusion within the Mesoporous Solid MIL-101 on Hydrogen Storage Performance. *Langmuir*, **2010**, *26*, 11283-11290
- [30] von Zeppelin, F.; Haluška, M., and Hirscher, M., Thermal Desorption Spectroscopy as a Quantitative Tool to Determine the Hydrogen Content in Solids. *Thermochim. Acta*, **2003**, *404*, 251-258

